

Contrast-Enhanced Ultrasound and Strain Elastography for Differentiating Benign and Malignant Parotid Tumors

Kontrastverstärkter Ultraschall und Strain-Elastografie zur Differenzierung benigner und maligner Parotistumore



Authors

LiuHong Shi¹, Dingting Wu², Xu Yang³, Caixin Yan¹, Pintong Huang¹

Affiliations

- 1 Department of Ultrasound in Medicine, Zhejiang University School of Medicine Second Affiliated Hospital, Hangzhou, China
- 2 Nutrition Division, The Fourth Affiliated Hospital Zhejiang University School of Medicine, Yiwu, China
- 3 Pathology, Zhejiang University School of Medicine First Affiliated Hospital, Hangzhou, China

Key words

contrast-enhanced ultrasound, strain elastography, benign parotid tumors, malignant parotid tumors

received 03.02.2022

accepted 21.05.2022

published online 02.02.2023

Bibliography

Ultraschall in Med 2023; 44: 419–427

DOI 10.1055/a-1866-4633

ISSN 0172-4614

© 2023. The Author(s).

This is an open access article published by Thieme under the terms of the Creative Commons Attribution-NonDerivative-NonCommercial-License, permitting copying and reproduction so long as the original work is given appropriate credit. Contents may not be used for commercial purposes, or adapted, remixed, transformed or built upon. (<https://creativecommons.org/licenses/by-nc-nd/4.0/>).

Georg Thieme Verlag KG, Rüdigerstraße 14,
70469 Stuttgart, Germany

Correspondence

Dr. Pintong Huang
Zhejiang University School of Medicine Second Affiliated Hospital
Department of Ultrasound in Medicine, Rd Jiefang 88,
310009 Hangzhou, China
huangpintong@zju.edu.cn

ABSTRACT

Objectives Preoperative differentiation between benign parotid tumors (BPT) and malignant parotid tumors (MPT) is crucial for treatment decisions. The purpose of this study was to investigate the benefits of combining contrast-enhanced ul-

trasound (CEUS) and strain elastography (SE) for preoperative differentiation between BPT and MPT.

Methods A total of 115 patients with BPT (n = 72) or MPT (n = 43) who underwent ultrasound (US), SE, and CEUS were enrolled. US and CEUS features and the elasticity score were evaluated. Receiver operating characteristic curve (ROC) analysis was used to assess the diagnostic performance of SE, CEUS, and SE + CEUS with respect to identifying MPT from BPT.

Results Solitary presentation, larger diameter, irregular shape, ill-defined margin, heterogeneous echogenicity, and calcification on US and higher elasticity score on SE had a significant association with malignancy. MPT also presented an unclear margin, larger size after enhancement, and “fast-in and fast-out” pattern on CEUS. The combination of SE and CEUS was effective for differentiating MPT from BPT (AUC: 0.88, 0.80–0.95), with a sensitivity of 86.0%, specificity of 88.9%, and accuracy of 87.8%, which were significantly higher than the values for SE (AUC: 0.75, 0.66–0.85) and CEUS (AUC: 0.82, 0.73–0.91) alone.

Conclusion The combination of CEUS and SE is valuable for distinguishing MPT from BPT.

ZUSAMMENFASSUNG

Ziel Die präoperative Differenzierung zwischen benignen Parotistumoren (BPT) und malignen Parotistumoren (MPT) ist maßgeblich für die Behandlungsentscheidung. Ziel dieser Studie war es, den Nutzen einer Kombination aus kontrastverstärktem Ultraschall (CEUS) und Strain-Elastografie (SE) zur präoperativen Differenzierung von BPT und MPT zu untersuchen.

Methoden Insgesamt wurden 115 Patienten mit BPT (n = 72) oder MPT (n = 43) eingeschlossen, die sich einer Ultraschalluntersuchung (US), SE und CEUS unterzogen. US- und CEUS-Merkmale sowie der Elastizitäts-Score wurden ausgewertet. Mit Hilfe der ROC-Analyse (Receiver Operating Characteristic Curve) wurde die diagnostische Leistung von SE, CEUS und SE + CEUS im Hinblick auf die Differenzierung von MPT und BPT bewertet.

Ergebnisse Solitäres Auftreten, größerer Durchmesser, unregelmäßige Form, schlecht definierter Rand, heterogene

Echogenität und Verkalkung auf US und ein höherer Elastizitätswert in der SE standen in einem signifikanten Zusammenhang mit Malignität. MPT zeigen auch einen unklaren Rand, einen größeren Umfang nach dem Enhancement und ein „Fast-in und Fast-out“-Muster im CEUS. Die Kombination von SE und CEUS war effektiv, um MPT und BPT zu differenzieren

(AUC: 0,88; 0,80–0,95), mit einer Sensitivität von 86,0%, einer Spezifität von 88,9% und einer Genauigkeit von 87,8% – diese Werte waren signifikant höher als die für SE (AUC: 0,75; 0,66–0,85) und CEUS (AUC: 0,82; 0,73–0,91) allein.

Schlussfolgerung Die Kombination von CEUS und SE ist wertvoll, um MPT von BPT zu differenzieren.

Introduction

Salivary gland tumors are uncommon, representing about 2–6% of all head and neck tumors. Parotid tumors account for approximately 80% of salivary gland tumors, with about 80% being benign [1, 2]. The therapy and prognosis are completely different between benign parotid tumors (BPT) and malignant parotid tumors (MPT) [3]. Therefore, accurate preoperative identification of MPT is essential for an aggressive approach and prognostic evaluation.

High-resolution ultrasound (US) is widely used for the initial assessment of parotid lesions, due to the simple, real-time, cost-effective, and non-radiated advantages [4]. US can determine the location, size, shape, margin, echogenicity of lesions, and lymph node involvement, which is useful in the differentiation of malignant lesions from benign ones [4, 5]. However, the accurate preoperative diagnosis of histopathology remains challenging.

Strain elastography (SE) and contrast-enhanced ultrasound (CEUS) are innovative and effective diagnostic tools that could provide additional information in the differentiation between benign and malignant lesions [6, 7]. SE shows the relative tissue elasticity and stiffness within a selected region of interest and is valuable for predicting malignancy [8]. CEUS is a novel technology to dynamically evaluate the microvessels and perfusion kinetics of lesions and is considered to be a powerful method in distinguishing malignant parotid lesions from benign ones [9]. However, the predictive value of SE combined with CEUS remains unclear. The present study is aimed to investigate the diagnostic accuracy of SE combined with CEUS in identifying malignant parotid tumors.

Materials and methods

Patients

This retrospective study was approved by the Ethics Committee of our institution. Written informed consent was waived for each patient. Patients were consecutively identified after searching the pathology database of our institution from January 2017 to May 2021. The inclusion criteria were as follows: (1) patients with a definitive diagnosis of BPT or MPT proven by biopsy or surgery; (2) patients simultaneously underwent conventional US, SE, and CEUS before treatment. 136 patients who met these criteria were enrolled in this study. The exclusion criteria were as follows: (1) images unsatisfactory for analysis because stored images were not enough to obtain required data ($n = 14$); (2) patients with secondary parotid carcinomas (metastatic tumors) or lymphoma

($n = 7$). Finally, a total of 115 patients were analyzed. When patients had multiple nodules, the largest nodule was selected.

US equipment and contrast agent

All ultrasonography examinations were performed using the My-Lab 90 (Esaote, Genoa, Italy; equipped with an L523 linear-array transducer for US and SE and L522 transducer for CEUS) and Resona 7 (Mindray, Shenzhen, China; equipped with an L14–5WU linear-array transducer for US and SE and L11–3U transducer for CEUS) US equipment. Sulfur hexafluoride (SonoVue; Bracco, Milan, Italy) was used as the contrast agent.

Conventional US

Conventional US was performed to scan the parotid gland lesions in multi-sections to obtain complete images of the lesions and surrounding normal tissues. US features were observed for each parotid lesion, including the number of lesions (single or multiple), size (the maximum diameter on US), shape (regular, lobulated, or irregular), margin (well-defined or poorly defined based on the boundary of the lesion and adjacent normal tissue), calcification, echogenicity (compared with the surrounding parotid tissue, classified as hypoechoic, hyperechoic, or isoechoic), cystic areas, and echotexture (homogeneous or heterogeneous). The blood flow of lesions was visualized by color Doppler ultrasonography (CDS). According to Alder's method [10], vascularity was graded as Grade 0 (no blood flow signal), Grade I (a small amount of blood flow, with 1–2 point-like or rod-like vessels), Grade II (a medium amount of blood flow, with 3–4 point-like vessels or a single long vessel), and Grade III (rich blood flow, with ≥ 5 punctate vessels or two long vessels).

SE examination and image analysis

SE was performed with light pressure while placing the probe vertically on the skin surface and gentle adjustment of pressure to acquire high-quality elastic images with the real-time quality indicator for optimal compression. The elastogram and grayscale images were simultaneously displayed on the screen with the region of interest including the mass and sufficient surrounding parotid tissue. The stiffness of the tissue was visualized by a continuum of color from green (soft tissue) to red (hard tissue).

According to the five-point scoring system [11], SE scores were classified as follows: a score of 1 indicated even strain for the entire lesion (homogeneously green), a score of 2 indicated strain in most areas of the lesion (predominantly green with a few red), a score of 3 indicated strain at the periphery of the lesion with sparing in the center (predominantly red with a few green), a score of

4 indicated no strain in the whole lesion (completely red), and a score of 5 indicated no strain in the whole lesion or the surrounding tissue (red area is larger than the lesion on conventional US). A lesion with an elasticity score > 3 was considered a malignancy.

CEUS examination and image analysis

CEUS examination was performed using the same equipment with a “low” mechanical index (0.07–0.09) and 4.8 ml (“1 vial”) of SonoVue. The suspension of SonoVue (25 mg, lyophilized powder) and saline solution (5 ml, 0.9% sodium chloride) were prepared and shaken uniformly. The SonoVue suspension was injected intravenously and then washed with 10 ml of saline. The timer on the ultrasound instrument was started and the entire imaging acquisition lasted at least 120 s.

CEUS features were analyzed by reviewing the cine loops as follows: i) enhancement degree was classified as low, equal, or high intensity (compared with the surrounding parotid tissue at the same level); ii) margin enhancement was classified as clear or unclear based on the clarity of the boundary between the lesion and adjacent normal tissue after enhancement; iii) ring enhancement was categorized as absent or present based on the appearance of a high-brightness ring around the lesion; iv) enhancement size was defined as larger or similar based on the size of the enhanced lesion compared with the lesion size on conventional US; v) enhancement texture was defined as homogeneous or heterogeneous based on the enhancement distribution of the lesion; vi) echo-free area was classified as absent or present based on the appearance of the perfusion area without contrast agent; vii) enhancement patterns included fast-in and fast-out, fast-in and slow-out, slow-in and fast-out, and slow-in and slow-out according to the time of contrast agent entering into the lesion and subsiding compared with surrounding parotid tissue. On CEUS, lesions with more than one suspicious feature (including unclear margin, larger size, and fast-in/fast-out) were considered malignant. On SE combined with CEUS, more than one suspicious CEUS features and/or a high elasticity score (> 3) indicated malignancy. Two radiologists (with > 8 years of experience in head and

neck US) independently reviewed these images and loops and were blinded to the clinical and pathological patient data. Different points were discussed to reach consensus.

Statistical analysis

All statistical analyses were performed with the SPSS software (version 20; SPSS Inc, Chicago, IL, USA). Continuous variables were showed as mean ± standard deviation (SD), categorical variables were presented as the number of cases. Independent t-test was used to compare continuous variables between two groups. Chi-square test or Fisher’s exact test was applied to compare categorical variables. The interobserver agreement between the two radiologists was assessed using the kappa statistic [12]. Receiver operating characteristic (ROC) curves were analyzed to evaluate the diagnostic sensitivity, specificity, positive predictive value (PPV), and negative predictive value (NPV) of SE, CEUS, and the combination of SE and CEUS. Areas under the ROC curves (AUC) with 95% confidence intervals (CI) were also calculated. A P-value < 0.05 was considered to be a statistically significant difference.

Results

Clinical and histopathological characteristics

The histopathological diagnosis of these parotid tumors was summarized in ► **Table 1**. A total of 115 patients with benign (n = 72, 39 males and 33 females) and malignant (n = 43, 22 males and 21 females) parotid tumors were enrolled. The average ages of patients with BPT or MPT were 57.5 years and 58.7 years, respectively. The demographic data is summarized in ► **Table 2**.

Conventional US features

The conventional US features are presented in ► **Table 2** and ► **Fig. 1**, ► **Fig. 2**. All parotid tumors were hypoechoic (► **Fig. 1A** and ► **Fig. 2A**). In patients with MPT, only two patients (4.7%) had

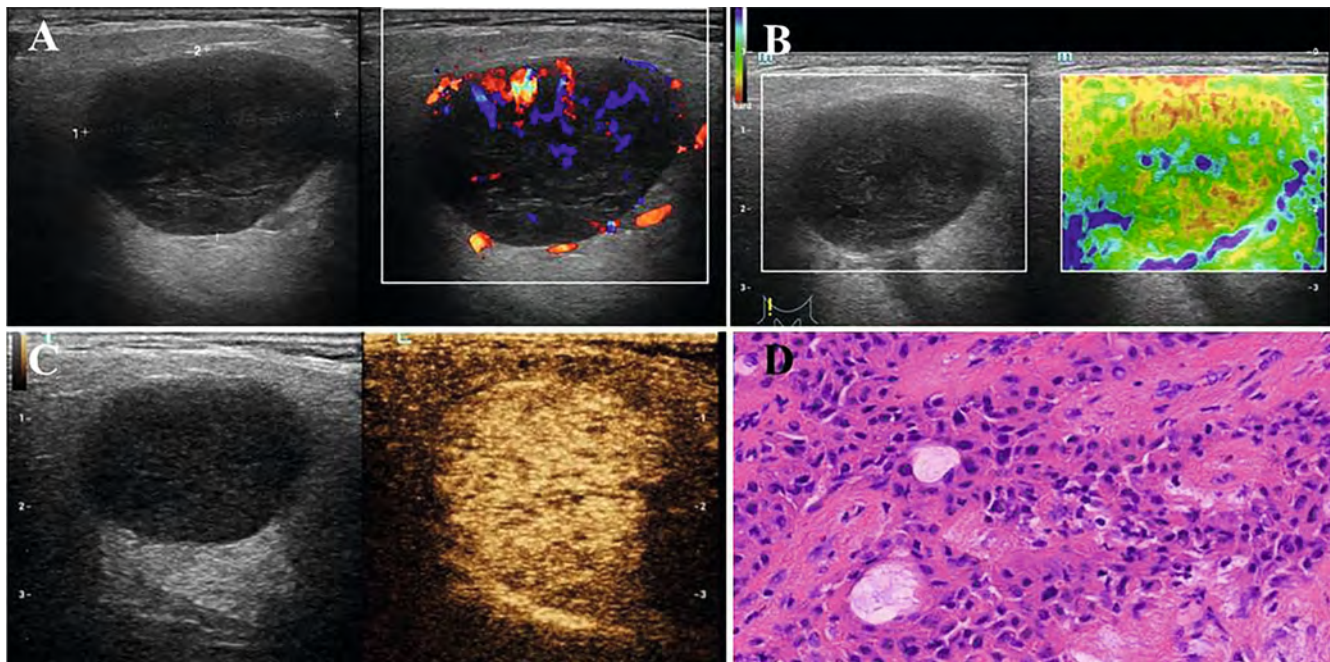
► **Table 1** Histopathological diagnosis of benign and malignant parotid tumors (n = 115).

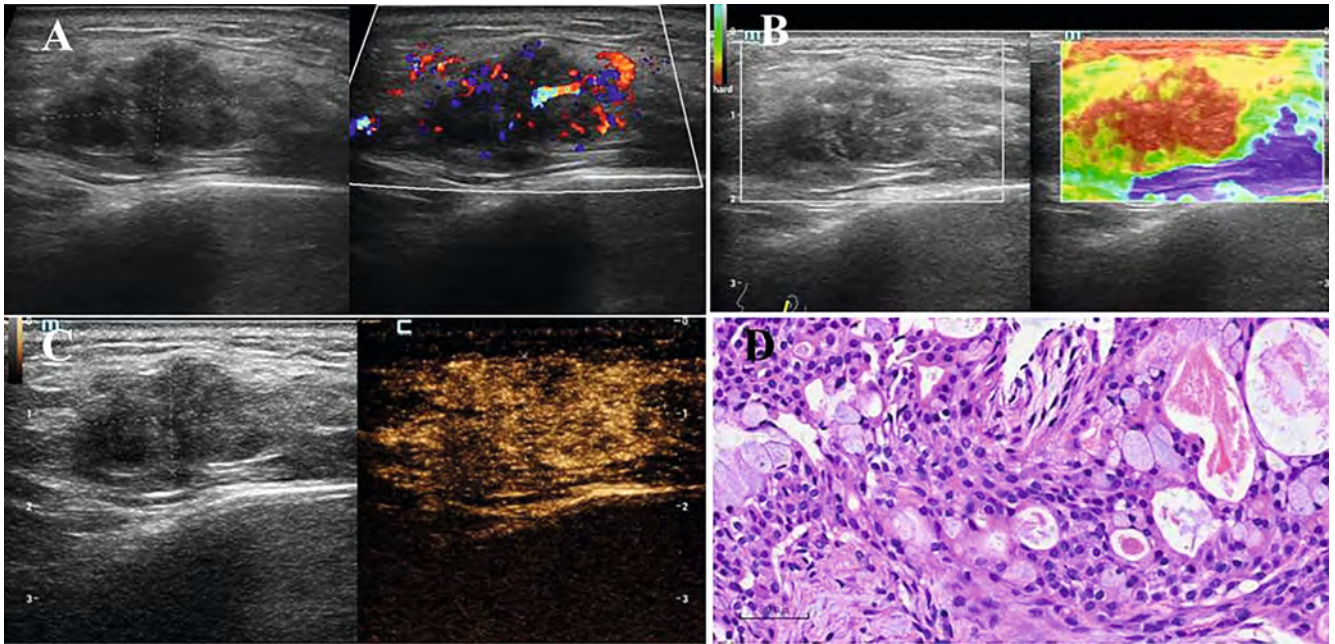
Benign (n = 72)	Number	Malignant (n = 43)	Number
Pleomorphic adenoma	36	Mucoepidermoid carcinoma	8
Warthin tumor	30	Adenoid cystic carcinoma	8
Basal cell adenoma	4	Salivary duct carcinoma	7
Oncocytoma	2	Adenocarcinoma, NOS	7
		Acinic cell carcinoma	5
		Squamous cell carcinoma	4
		Lymphoepithelial carcinoma	2
		Carcinosarcoma	1
		Basal cell adenocarcinoma	1

NOS: not otherwise specified

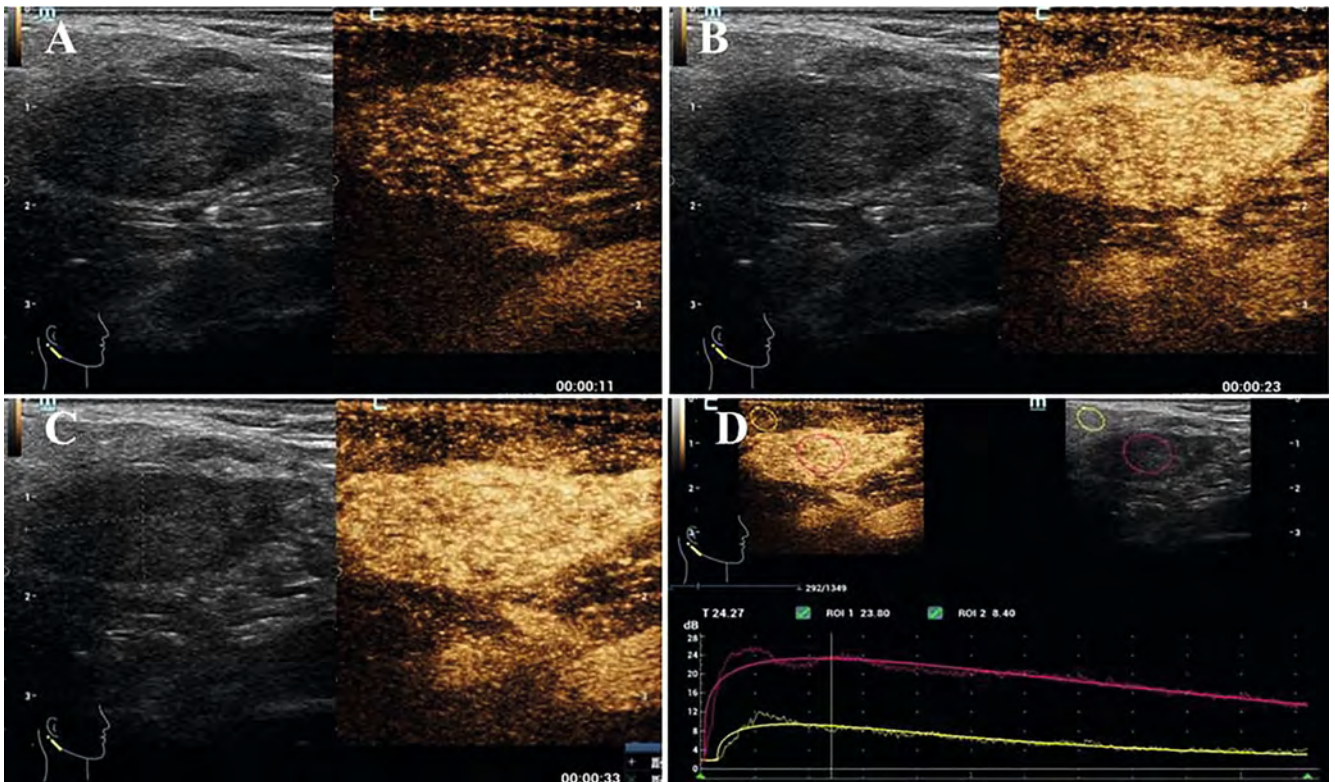
► **Table 2** Clinical and US characteristics of patients with benign and malignant parotid tumors (n = 115).

Features	Benign (n = 72)	Malignant (n = 43)	P-value
Age (year)	57.5 ± 15.2	58.7 ± 19.2	0.716
Sex			0.755
Male	39	22	
Female	33	21	
Number of lesions			0.018
Single	57	41	
Multiple	15	2	
Maximum diameter (mm)	26.81 ± 9.07	35.03 ± 13.04	< 0.001
Shape			< 0.001
Regular	41	3	
Lobulated	22	7	
Irregular	9	33	
Margin			< 0.001
Well-defined	64	13	
Poorly defined	8	30	
Echogenicity			Not available
Hypoechoic	72	43	
Hyper-/isoechoic	0	0	
Echotexture			0.021
Homogeneous	34	11	
Heterogeneous	38	32	
Calcification (yes/no)	3/69	15/28	< 0.001
Cystic areas (yes/no)	18/54	11/32	0.945
Blood flow grade			0.252
0-I	24	10	
II-III	48	33	

► **Fig. 1** Images of pleomorphic adenoma in the right lobe of a 57-year-old male. **A** Conventional ultrasound and Color Doppler ultrasonography showed a hypoechoic and regular mass with a well-defined margin and abundant blood flow signals (Grade III). **B** The SE score was 2. **C** The CEUS indicated the lesion with a clear margin and homogeneous hyperenhancement. **D** Pathological image of the lesion was a pleomorphic adenoma.



► **Fig. 2** Images of mucoepidermoid carcinoma in the left lobe of a 53-year-old female. **A** Conventional ultrasound and color Doppler ultrasonography showed a hypoechoic and irregular mass with an ill-defined margin and marked vascularity (Grade III). **B** The SE score was 5. **C** CEUS showed the lesion with an unclear margin, larger size after enhancement, and heterogeneous hyperenhancement. **D** Pathological image of the lesion was a mucoepidermoid carcinoma. SE: strain elastography; CEUS: contrast-enhanced ultrasound.



► **Fig. 3** Images of Warthin tumor in the right lobe of a 53-year-old male. The CEUS showed the lesion with a clear margin, homogeneous hyperenhancement, and the perfusion pattern of “fast-in and slow-out” (**A**-early phase, **B**-middle phase, and **C**-late phase). **D** Time-intensity curve analysis showed the perfusion kinetics of the lesion (red line) and surrounding tissue (yellow line). CEUS: contrast-enhanced ultrasound.

► **Table 3** SE and CEUS characteristics of patients with benign and malignant parotid tumors (n = 115).

Features	Benign (n = 72)	Malignant (n = 43)	P-value
Elasticity score			<0.001
>3	7	26	
≤3	65	17	
Enhancement intensity			0.423
Low or equal	20	15	
High	52	28	
Margin enhancement			<0.001
Clear	51	8	
Unclear	21	35	
Ring enhancement			0.013
Absent	59	42	
Present	13	1	
Size enhancement			<0.001
Larger	5	20	
Similar	67	23	
Enhancement texture			0.123
Homogeneous	34	14	
Heterogeneous	38	29	
Echo-free area			0.631
Absent	50	28	
Present	22	15	
Enhancement mode			<0.001
Fast-in and fast-out	10	25	
Fast-in and slow-out	25	6	
Slow-in and fast-out	23	7	
Slow-in and slow-out	12	4	

SE: strain elastography; CEUS: contrast-enhanced ultrasound

multiple nodules. The maximum diameter of MPT was significantly larger than that of BPT (35.03 ± 13.04 mm in MPT vs 26.81 ± 9.07 mm in BPT, $P < 0.001$). Irregular shape (76.7%), poorly defined margin (69.8%), and calcification (34.9%) were significantly associated with malignancy ($P < 0.001$). Malignant parotid tumors more frequently had a heterogeneous echotexture (74.4%, $P = 0.021$). With respect to the appearance of cystic areas and blood flow abundance, there was no significant difference ($P > 0.05$).

SE and CEUS features

The SE and CEUS features were presented in ► **Table 3** and ► **Fig. 1**, ► **Fig. 2**, ► **Fig. 3**, ► **Fig. 4**. Malignancy was significantly associated with a high elastic score (60.5%, $P < 0.001$, ► **Fig. 1B** and ► **Fig. 2B**). The perfusion kinetics of CEUS were observed. Unclear margin (35/43, 81.4%) and larger size (20/43, 46.5%) after enhancement were significantly associated with malignancy ($P < 0.001$, ► **Fig. 1C** and ► **Fig. 2C**). Ring enhancement (2.3%) was rare in malignant lesions. Among the malignant lesions, most lesions (25/43, 58.1%) had a “fast-in and fast-out” pattern (► **Fig. 3**). Among the benign lesions, 25 (34.7%) had a “fast-in and slow-out” and 23 (31.9%) had “slow-in and fast-out” pattern (► **Fig. 4**). Most benign lesions (72.2%) and malignant lesions (65.1%) were hyperenhanced. There were no significant differ-

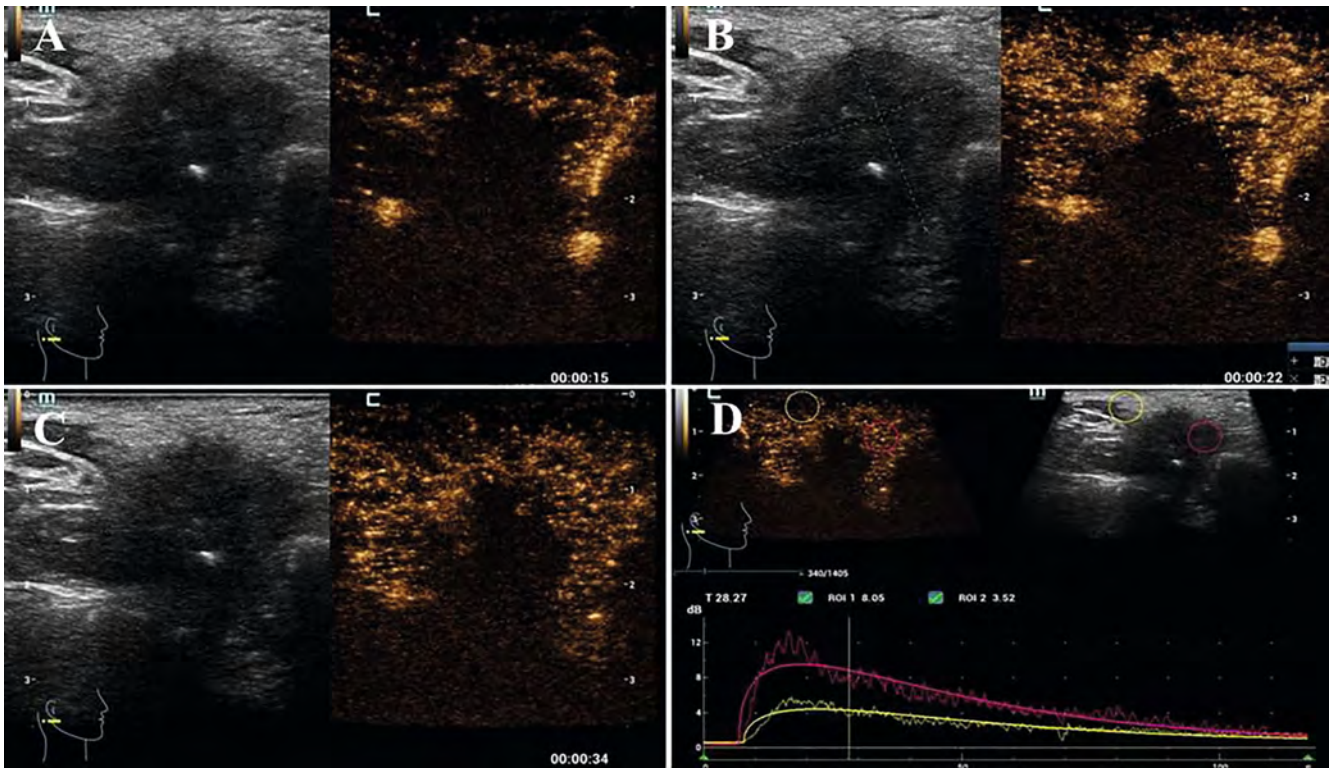
ences in enhancement intensity, enhancement texture, and echo-free area ($P > 0.05$). The multimodal diagnostic pathway was presented in ► **Fig. 5**. The interobserver consistency for the combination of SE and CEUS was 0.89 (95% CI 0.79–0.98), indicating a high level of interobserver reliability.

ROC analysis

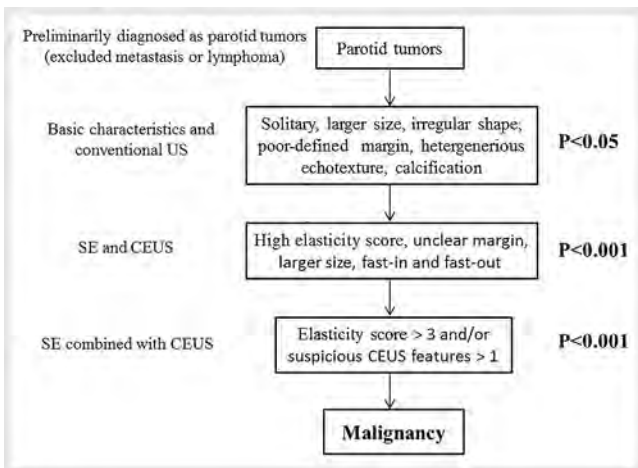
ROC analysis was performed to evaluate the diagnostic value of SE, CEUS, and the combination of SE and CEUS (SE+CEUS) in distinguishing MPT from BPT. The AUC of SE+CEUS (0.88, 95% CI: 0.80–0.95) was significantly higher than that of SE (0.75, 95% CI: 0.66–0.85) and CEUS (0.82, 95% CI: 0.73–0.91) alone. The corresponding sensitivity, specificity, and accuracy were 86.0%, 88.9%, and 87.8% for SE+CEUS; 60.5%, 90.1% and 79.1% for SE; 72.1%, 91.7%, and 84.3% for CEUS (► **Table 4**, ► **Fig. 6**). The combination of SE and CEUS exhibited preferable diagnostic value in differentiating MPT from BPT.

Discussion

With regard to parotid tumors, pleomorphic adenoma (PA) and Warthin tumor (WT) comprise the vast majority (83–93%) of all benign tumors [13]. Malignant lesions are relatively rare and



► **Fig. 4** Images of adenocarcinoma-not otherwise specified (NOS) in the right lobe of a 76-year-old male. CEUS showed the lesion with an unclear margin and larger size after enhancement, echo-free area, heterogeneous hyperenhancement, and the perfusion pattern of “fast-in and fast-out” (A-early phase, B-middle phase, and C-late phase). D Time-intensity curve analysis showed the perfusion kinetics of the lesion (red line) and surrounding tissue (yellow line). CEUS: contrast-enhanced ultrasound.



► **Fig. 5** Multimodal diagnostic pathway. Basic clinical characteristics and conventional US distinguished malignant from benign tumors initially. SE and CEUS showed the elasticity and microvessels of lesions and further differentiated the lesions. US: ultrasound; SE: strain elastography; CEUS: contrast-enhanced ultrasound.

have a variety of histopathological subtypes. The preoperative differentiation between benign and malignant lesions has major clinical significance for defining the treatment plan and selecting the appropriate surgical scheme. Previous studies have shown that sonoelastography and CEUS could provide useful and progressive

information for accurate diagnosis between tumors in many organs, including thyroid, breast, and parotid [14, 15, 16, 17].

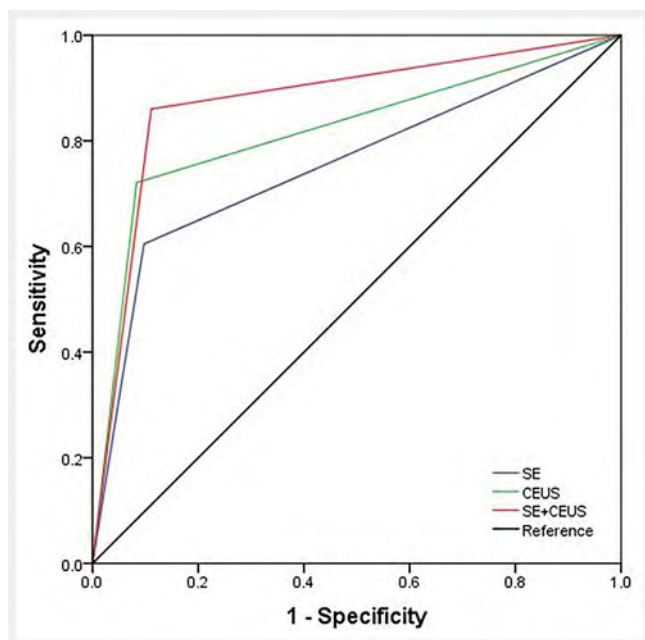
Sonoelastography is an innovative diagnostic tool for assessing tissue elasticity and stiffness [11]. Several studies have explored the value of sonoelastography in distinguishing between benign and malignant parotid tumors. Although malignancies should be theoretically stiffer, the status remains complicated. Known data on the value of sonoelastography in diagnosing malignant parotid tumors showed a wide range in sensitivity (38–100%) and specificity (26–97%) [18, 19, 20]. A meta-analysis revealed a low pooled sensitivity and specificity for differentiating benign and malignant parotid lesions with an AUC of 0.77 [21]. Our study also showed that SE alone had a sensitivity of 60.5% and a specificity of 90.1% with an AUC of 0.75. The value of SE alone is limited and is not satisfactory for the differential diagnosis.

CEUS represents another relatively new promising ultrasound technique for the head and neck to describe the microvasculature of lesions [22, 23]. Numerous studies have reported that CEUS can differentiate between benign and malignant lesions [17, 24]. Malignant characteristics include an unclear margin, inhomogeneous vascularization, and uneven distribution of circulating beds [7]. According to the present study, an unclear margin (81.4%), larger size after enhancement (46.5%), and a pattern of “fast-in/fast-out” (58.1%) were significantly associated with malignant parotid tumors. These might be attributed to invasive growth, the number of increased blood vessels, abnormal arteriovenous fistula, and changes of vascular permeability [25]. The

► **Table 4** Diagnostic performance of SE, CEUS, and combination of SE and CEUS for distinguishing between benign and malignant parotid tumors.

Features	AUC (95 % CI)	Accuracy, %	Sensitivity, %	Specificity, %	PPV, %	NPV, %	P-value
SE	0.75 (0.66–0.85)	79.1	60.5	90.1	78.8	79.3	<0.001
CEUS	0.82 (0.73–0.91)	84.3	72.1	91.7	83.7	84.6	<0.001
SE+CEUS	0.88 (0.80–0.95)	87.8	86.0	88.9	82.2	91.4	<0.001

SE: elasticity score > 3; CEUS: > 1 suspicious CEUS features; SE+CEUS: elasticity score > 3 and/or > 1 suspicious CEUS features. SE: strain elastography; CEUS: contrast-enhanced ultrasound; AUC: area under the receiver operating characteristic curve; CI: confidence interval; PPV: positive predictive value; NPV: negative predictive value



► **Fig. 6** ROC curve of SE and CEUS for differentiating malignant parotid tumors. The AUC with respect to predicting malignancy was 0.75 for SE, 0.82 for CEUS, and 0.88 for SE and CEUS. ROC: receiver operating characteristics; SE: strain elastography; CEUS: contrast-enhanced ultrasound; AUC: area under curve.

perfusion patterns of benign tumors in our study were mostly “fast-in/slow-out” and “slow-in/fast-out”, which is similar to the previous study [26]. Previous studies also revealed that heterogeneous enhancement indicated the presence of malignant lesions [7, 9]. However, there was no significant difference in heterogeneous enhancement of benign (52.8%) and malignant (67.4%) parotid tumors in the present study. This may be due to the inclusion of the relatively small number of malignant lesions and all types of malignant lesions (primary, secondary carcinomas and lymphomas) in previous studies.

The SE and CEUS techniques showed statistically significant differences in elasticity score and enhancement features between benign and malignant parotid lesions, evidenced by several previous studies [17, 21, 27]. However, the number of primary malignant tumors (less than 15 cases) was relatively small, and the elastosonographic methods were diversified and inconsistent in

previous studies [9, 17, 27]. In addition, overlap characteristics in benign and malignant lesions have been found in the use of SE and CEUS alone. Some studies had shown that combining sonoelastography and CEUS improved the diagnostic efficacy of malignant lesions in multiple organs [28, 29]. However, the diagnostic power of SE plus CEUS has not been assessed in the parotid. In the present study, SE combined with CEUS significantly increased the sensitivity of malignant lesions, and the specificity did not significantly decrease. The excellent diagnostic efficiency was achieved with an AUC of 0.88, accompanied by a sensitivity of 86.0% and a specificity of 88.9%. The diagnostic value was proven to be higher than that of either technique alone. These findings indicate that the combination of SE and CEUS significantly improves the diagnostic accuracy of preoperative malignant parotid tumors. In addition, the excellent interobserver agreement might be because the two radiologists reviewing images and loops were very experienced.

There were several limitations in this study. Firstly, the imaging features of WT and PA are notably different. However, the differentiation of malignant tumors from benign ones was assumed to be more important, so we did not analyze PA and WT. Secondly, the quantitative analysis of CEUS was not performed in some cases and was not convenient to be used routinely in clinical practice. Thus, we did not perform the quantitative CEUS analysis, which needs to be evaluated in the future. Thirdly, this is a retrospective study involving a single center. In addition, some patients were excluded due to a lack of complete imaging data. These factors might lead to an unavoidable selection bias.

In conclusion, the present study indicated that the combination of SE and CEUS significantly improved the diagnostic accuracy of malignant parotid tumors compared with SE or CEUS alone.

Funding

Medical and Health Research Project of Zhejiang Province | <http://dx.doi.org/10.13039/501100017531> (2021KY703) | Natural Science Foundation of Zhejiang Province | <http://dx.doi.org/10.13039/501100004731> (LQ20H180011)

Conflict of Interest

The authors declare that they have no conflict of interest.

References

- [1] Vasconcelos AC, Nör F, Meurer L et al. Clinicopathological analysis of salivary gland tumors over a 15-year period. *Braz Oral Res* 2016; 30. doi:10.1590/1807-3107BOR-2016.vol30.0002
- [2] Fu JY, Wu CX, Shen SK et al. Salivary gland carcinoma in Shanghai (2003–2012): an epidemiological study of incidence, site and pathology. *BMC Cancer* 2019; 19: 350. doi:10.1186/s12885-019-5564-x
- [3] Thielker J, Grosheva M, Ihrler S et al. Contemporary Management of Benign and Malignant Parotid Tumors. *Front Surg* 2018; 5: 39. doi:10.3389/fsurg.2018.00039
- [4] Gritzmann N, Rettenbacher T, Hollerweger A et al. Sonography of the salivary glands. *Eur Radiol* 2003; 13: 964–975. doi:10.1007/s00330-002-1586-9
- [5] Howlett DC. High resolution ultrasound assessment of the parotid gland. *Br J Radiol* 2003; 76: 271–277. doi:10.1259/bjr/33081866
- [6] Sigrist RMS, Liao J, Kaffas AE et al. Ultrasound Elastography: Review of Techniques and Clinical Applications. *Theranostics* 2017; 7: 1303–1329. doi:10.7150/thno.18650
- [7] David E, Cantisani V, De Vincentiis M et al. Contrast-enhanced ultrasound in the evaluation of parotid gland lesions: an update of the literature. *Ultrasound* 2016; 24: 104–110. doi:10.1177/1742271X15626611
- [8] Cantisani V, David E, Barr RG et al. US-Elastography for Breast Lesion Characterization: Prospective Comparison of US BIRADS, Strain Elastography and Shear wave Elastography. *Ultraschall in Med* 2021; 42: 1533–1540. doi:10.1055/a-1134-4937
- [9] Sultan SR, Alkharaji M, Rajab SH. Diagnosis of parotid gland tumours with Contrast-Enhanced Ultrasound: a systematic review and meta-analysis. *Med Ultrason* 2021. doi:10.11152/mu-3119
- [10] Adler DD, Carson PL, Rubin JM et al. Doppler ultrasound color flow imaging in the study of breast cancer: preliminary findings. *Ultrasound Med Biol* 1990; 16: 553–559. doi:10.1016/0301-5629(90)90020-d
- [11] Itoh A, Ueno E, Tohno E et al. Breast disease: clinical application of US elastography for diagnosis. *Radiology* 2006; 239: 341–350. doi:10.1148/radiol.2391041676
- [12] Landis JR, Koch GG. The measurement of observer agreement for categorical data. *Biometrics* 1977; 33: 159–174
- [13] Bradley PJ, McGurk M. Incidence of salivary gland neoplasms in a defined UK population. *Br J Oral Maxillofac Surg* 2013; 51: 399–403. doi:10.1016/j.bjoms.2012.10.002
- [14] Xi X, Gao L, Wu Q et al. Differentiation of Thyroid Nodules Difficult to Diagnose With Contrast-Enhanced Ultrasonography and Real-Time Elastography. *Front Oncol* 2020; 10: 112. doi:10.3389/fonc.2020.00729
- [15] Lee YJ, Kim SH, Kang BJ et al. Contrast-Enhanced Ultrasound for Early Prediction of Response of Breast Cancer to Neoadjuvant Chemotherapy. *Ultraschall in Med* 2019; 40: 194–204. doi:10.1055/a-0637-1601
- [16] Jia W, Luo T, Dong Y et al. Breast Elasticity Imaging Techniques: Comparison of Strain Elastography and Shear-Wave Elastography in the Same Population. *Ultrasound Med Biol* 2021; 47: 104–113. doi:10.1016/j.ultrasmedbio.2020.09.022
- [17] Mansour N, Bas M, Stock KF et al. Multimodal Ultrasonographic Pathway of Parotid Gland Lesions. *Ultraschall in Med* 2017; 38: 166–173. doi:10.1055/s-0035-1553267
- [18] Klintworth N, Mantsopoulos K, Zenk J et al. Sonoelastography of parotid gland tumours: initial experience and identification of characteristic patterns. *Eur Radiol* 2012; 22: 947–956. doi:10.1007/s00330-011-2344-7
- [19] Wierzbicka M, Kaluźny J, Szczepanek-Parulska E et al. Is sonoelastography a helpful method for evaluation of parotid tumors? *Eur Arch Otorhinolaryngol* 2013; 270: 2101–2107. doi:10.1007/s00405-012-2255-5
- [20] Mansour N, Stock KF, Chaker A et al. Evaluation of parotid gland lesions with standard ultrasound, color duplex sonography, sonoelastography, and acoustic radiation force impulse imaging – a pilot study. *Ultraschall in Med* 2012; 33: 283–288. doi:10.1055/s-0031-1299130
- [21] Zhang YF, Li H, Wang XM et al. Sonoelastography for differential diagnosis between malignant and benign parotid lesions: a meta-analysis. *Eur Radiol* 2019; 29: 725–735. doi:10.1007/s00330-018-5609-6
- [22] Wilson SR, Burns PN. Microbubble-enhanced US in body imaging: what role? *Radiology* 2010; 257: 24–39. doi:10.1148/radiol.10091210
- [23] Wei X, Li Y, Zhang S et al. Evaluation of microvascularization in focal salivary gland lesions by contrast-enhanced ultrasonography (CEUS) and Color Doppler sonography. *Clin Hemorheol Microcirc* 2013; 54: 259–271. doi:10.3233/CH-131732
- [24] Yang L, Zhao H, He Y et al. Contrast-Enhanced Ultrasound in the Differential Diagnosis of Primary Thyroid Lymphoma and Nodular Hashimoto's Thyroiditis in a Background of Heterogeneous Parenchyma. *Front Oncol* 2021; 10: 597975. doi:10.3389/fonc.2020.597975
- [25] Dvorak HF. Tumor Stroma, Tumor Blood Vessels, and Antiangiogenesis Therapy. *Cancer J* 2015; 21: 237–243. doi:10.1097/PP0.0000000000000124
- [26] Yan M, Xu D, Chen L et al. Comparative Study of Qualitative and Quantitative Analyses of Contrast-Enhanced Ultrasound and the Diagnostic Value of B-Mode and Color Doppler for Common Benign Tumors in the Parotid Gland. *Front Oncol* 2021; 11: 669542. doi:10.3389/fonc.2021.669542
- [27] Knopf A, Mansour N, Chaker A et al. Multimodal ultrasonographic characterisation of parotid gland lesions—a pilot study. *Eur J Radiol* 2012; 81: 3300–3305. doi:10.1016/j.ejrad.2012.01.004
- [28] Sui X, Liu HJ, Jia HL et al. Contrast-enhanced ultrasound and real-time elastography in the differential diagnosis of malignant and benign thyroid nodules. *Exp Ther Med* 2016; 12: 783–791. doi:10.3892/etm.2016.3344
- [29] Xiang LH, Yao MH, Xu G et al. Diagnostic value of contrast-enhanced ultrasound and shear-wave elastography for breast lesions of sub-centimeter. *Clin Hemorheol Microcirc* 2017; 67: 69–80. doi:10.3233/CH-170250